PROCEEDINGS OF SPIE

SPIEDigitalLibrary.org/conference-proceedings-of-spie

Monitoring of pulse signals with flexible paper-based graphene sensor

Mingzhe Wang, Jieyuan Zou, Siyuan Zeng, Yanqing Feng, Yang Shen, et al.

Mingzhe Wang, Jieyuan Zou, Siyuan Zeng, Yanqing Feng, Yang Shen, Yong You, "Monitoring of pulse signals with flexible paper-based graphene sensor," Proc. SPIE 12916, Third International Conference on Signal Image Processing and Communication (ICSIPC 2023), 129161P (20 October 2023); doi: 10.1117/12.3005132

SPIE.

Event: Third International Conference on Signal Image Processing and Communication (ICSIPC 2023), 2023, Kunming, China

Monitoring of pulse signals with flexible paper-based graphene sensor

Mingzhe Wang, Jieyuan Zou, Siyuan Zeng, Yanqing Feng*, Yang Shen, Yong You
School of Mathematics and Civil Engineering, Zhuhai College, Beijing Institute of Technology, Zhuhai 519088;
*Corresponding author e-mail: yq_feng@bitzh.edu.cn; 12057@bitzh.edu.cn

Abstract

Wearable flexible sensors are being increasingly designed for monitoring human health states. In this study, we optimized the preparation process of paper-based graphene and designed amplifier filter circuit to sense weak pulse signals with high sensitivity (0~300Pa) and fast response time (<1ms). We further used a convolutional neural network (CNN) as the recognition method to analyze the collected pulse signals. We successfully achieved the recognition and classification of three signals (Cun, guan, chi, and Sport) with an accuracy of 85.79% in the training set and an accuracy of 80% in the testing set. Our research offers new possibilities for the wide application of paper-based graphene sensors in medical diagnosis and health monitoring.

Key words：Wearable flexible sensors； graphene； pulse signals; convolutional neural network

1. Introduction

Nowadays, flexible sensors have become widely employed to monitor vital signs for medical applications[1] such as pulse, breathing and heartbeat due to their versatility and adaptability[2]. For pulse signals, there are Cun, Guan, and Chi commonly found in Chinese medical theory[3], however, identifying and interpreting these three stable and accurate signals can be challenging, as the differences between signals are sligh. New materials, graphene can be combined with other materials as flexible sensors with high sensitivity and high precision as its excellent electro-mechanical properties[4,5]. However, most graphene sensors fabricated methods like chemical vapor deposition (CVD) [6] are complex, time-consuming, and expensive, making it challenging for real-time monitoring applications [7].

Here, we propose a low-cost, portable, and lightweight paper-based graphene flexible sensor[8] to achieve high sensitivity measurement of pulse signals, which has a sensitivity range (0~300 Pa) and response time (<1 ms) suitable for deriving stable pulse wave signals. We obtain and distinguish three pulse signals (Cun, Guan, and Chi) by constructing signal acquisition and detection circuit. To address the subjectivity and large errors, we employed deep learning (CNN convolutional neural network)[9-11] to process Cun, Guan, Chi, and motion collected in experiment. This was done to classify and identify these four types of signals and correctly identify the pulse location. The CNN pulse recognition classification reached a final training set accuracy of 85.79% and a test set accuracy of 80%, providing a reliable reference for TCM pulse diagnosis. This approach improves the subjective error caused by manual classification and enables a more reliable pulse diagnosis.

2. Materials and Methods

2.1 Preparation process of paper-based graphene sensors

The modified Hummers method was utilized to synthesize graphene oxide[12], as illustrated in Fig. 1(a). To create aqueous and oil-based CO solutions with concentrations of 1, 2, 3, and 4, respectively, a 120 W ultrasonic device was employed. The solution was then sonicated at room temperature for 3-5 hours. Subsequently, a piece of paper towel measuring 2 cm × 2 cm (designated as CO_0T) was cut into small squares. These squares were soaked in varying concentrations of oil-based and water-based CO solutions for 4 hours. The wet CO_0T was removed and dried in an electric thermostatic drying oven at 100 ° C for 30 minutes to produce CO_1T. This process was then repeated as illustrated in Fig. 1(b) to yield subsequent samples CO_2T, CO_3T, CO_4T, and CO_5T. However, the fifth iteration resulted in some electrical conductivity for CO5T. Achieving these results required multiple experiments to regulate the immersion time, drying duration, and number of immersions for the paper-based films.

Third International Conference on Signal Image Processing and Communication (ICSIPC 2023),
edited by Gang Wang, Lei Chen, Proc. of SPIE Vol. 12916, 129161P
 · 0277-786X · doi: 10.1117/12.3005132

According to the conductive mechanism of conductive polymer composites[13], the conductivity experiences a sudden increase at the percolation threshold with highest sensitivity. In this experiment, we determined the percolation threshold of a paper-based film by adjusting the number of times the experimental paper soaked in the graphene solution and the drying time of the graphene paper-based film, so that the graphene contents on the paper base change. The conductivity of the resulting sensor were measured by a four-probe instrument (Fig. 1(c)) and we found that the conductivity was adversely affected by a small CO solution concentration and a limited number of immersions. As depicted in Fig. 1(h), a higher concentration of graphene solution results in stronger conductivity of the graphene paper-based film. Hence, a thin layer resistance, appropriate for achieving optimal device performance, needs to be selected. Furthermore, the conductivity of the graphene sensor is also influenced by the number of immersions as illustrated in Fig. 1(g). Within a limited range, the graphene paper substrate's conductivity is positively related to that of the graphene paper-based film. The conductivity of the graphene film decreases beyond a specific number of immersions, highlighting the threshold theory of the sensor sensing mechanism.

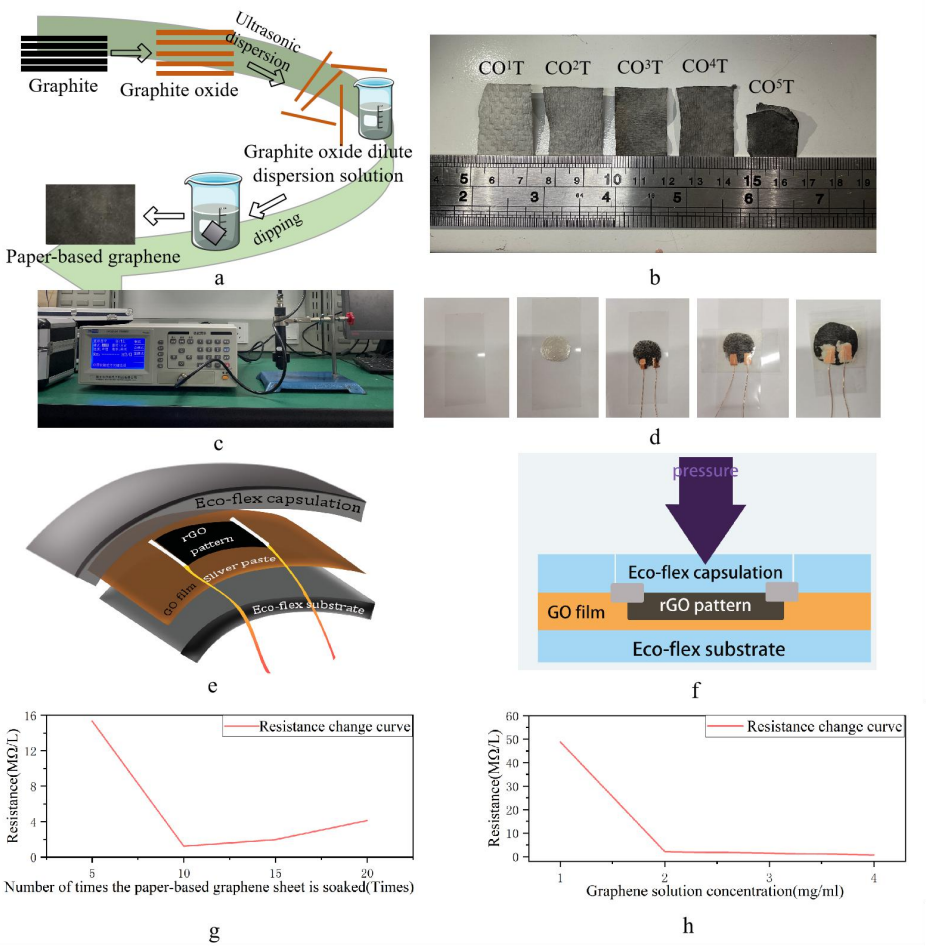

Figure 1 (a) Paper-based graphene flexible sensor preparation process; (b) Paper-based graphene flexible film specimens with different soaking times; (c) Four-probe method for measuring electrical conductivity instrument for paper-based graphene flexible sensor; (d) Paper-based graphene flexible sensor packaging process based on pet film; (e) Paper-based graphene flexible sensor model; (f) Principle of pressure change generated by the sensor after force (g) Graphene sensor electrical conductivity with-soaking times; (h) Graphene sensor electrical conductivity with graphene concentration curve.

2.2 Signal processing circuit

Energy storage bypass circuit (shown in Fig. 2(a)) was designed with a capacitor of 0.1 μF is connected between the power supply and ground[14] to stabilize the supply voltage and enhance the signal stability by bypassing the AC noise.

A second-stage amplifier filter circuit[15] is shown in Fig. 2(b) to amplify the signal by a factor of 100, which is

comprised of two 10-fold amplification circuits. The amplification factor Av of the operational amplifier can be determined using the formula:

$$Av = (1 + \frac{R_5}{R_4})(1 + \frac{R_9}{R_8})$$

Fig. 2(c) depicts a band-pass filter circuit in conjunction with the secondary amplifier circuit, which includes a low-pass filter with a cutoff frequency of 45 Hz and a high-pass filter with a cutoff frequency of 0.08 Hz, resulting in a dual filtering and amplification capability. The range of the high-pass filter W_1 was determined using the following equation:

$$W_1 = \frac{1}{2\pi Z_1 R_1}$$

The low-pass filter W_2 ranges as following:

$$W_2 = \frac{1}{2\pi Z_2 R_2}$$

Fig. 2(e) show lightweight and portable functionality with all modules integrated into the board.The USB-6363 data acquisition card from NI is a device used for data acquisition. With 24 acquisition channels, it conveniently enables array-based signal acquisition. The acquisition card is connected to the host computer, and the LabVIEW program's acquisition module is utilized to output the signal.

2.3 Paper-based graphene sensor performance test

We conducted a sensitivity test as depicted in Fig. 2(f) and 12000 data points were collected at a sampling rate of 3120. The sensor was subjected to the same pressure and time interval for each press, resulting in a stable square wave pattern in the graph. According to the formula $t = \frac{N}{f_s}$, where N represents the sampling point and f_s is the sampling frequency, the sensor takes 16ms to recover to its original state after receiving pressure. The sensor underwent pressure testing by applying forces of [50, 100, 150, 200, 250, 300] g to its surface, as illustrated in Fig. 2(g). As pressure gradually increased according to a specific rule, the waveform of the sensor demonstrably changed in regular intervals and the error remained within acceptable limits of 3%.

3. Data acquisition, processing and results analysis based on Machine Learning

Here, we invited 10 volunteers (ranging from 10 to 24 years old) to serve as subjects for our observation. During the measurement process, the exact location of the pre-marked Cun, Guan, and Chi signals was identified, and the equipment was closely fitted to the volunteer's wrist. The pulse waveform was collected using an oscilloscope shown in Fig. 3. We can see that all pulse cycles exhibited similar shapes and distinctive characteristic points. The oscilloscope acquisition frequency was divided into 10HZ, and 20,000 points were acquired each time.

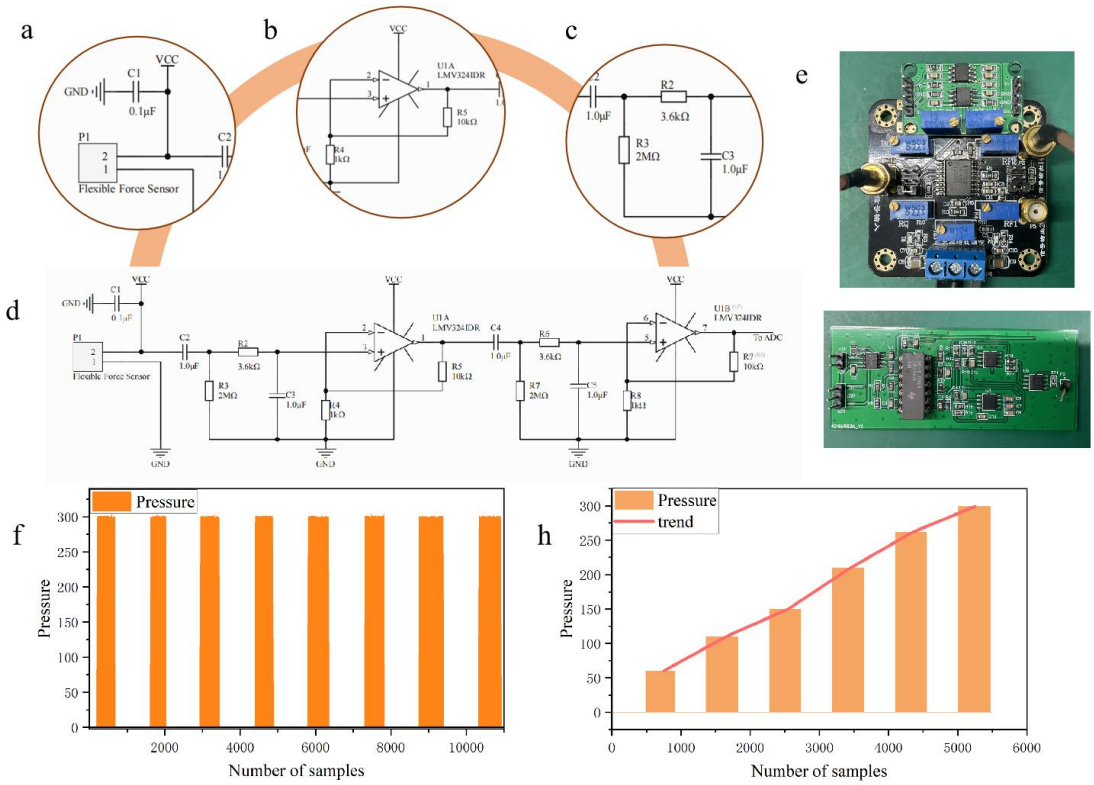

Figure 2. (a) Energy storage bypass circuit with an additional 0.1μF capacitor; (b) Signal secondary amplification circuit module; (c) Bandpass filter processing module; (d) Signal amplification and filter processing integrated circuit module; (e) Sensor IC modules (amplification, filtering) ;(f) Sensitivity test of the sensor(Same interval) ;(g) pressure change performance test

The sensor distinguished all three characteristic peaks of the pulse waveform from Cun, Guan, and Chi, and the 3D graph is shown in Fig. 4(a). The figure illustrates that the Guan signal has the highest pulse amplitude while the Chi signal has the lowest, same to the principles of traditional Chinese medicine[16,17] . In Fig. 4(b), the areas of the main wave and the reboot wave for the Cun signal and the Guan signal are compared. It can be seen that the upwave area of the Cun signal constitutes a significant portion of the pulse signal for one cycle, whereas, for the Guan signal, the reboot wave area accounts for most of the pulse signal for one cycle. To investigate the wrist pulse signals' characteristics, Fig. 4(c) plots the differences between Cun, Guan, and Chi at the same time, with the Chi signal represented by a brief and weak signal, the Cun signal by a rapid rhythm and smooth pulse, and the Guan signal by an undulating waveform.

We further use deep learning to process medical pulse signals, helping to locate the correct pulse site, explore different pulse characteristics, and promote the progress of smart medicine. We classifies and recognizes four types of signals - Cun, Guan, Chi, and motion - which improves recognition accuracy. The data is partitioned into training and validation sets at an 8:2 ratio, and augmented using both panning and scaling techniques exclusively on the training set. For each

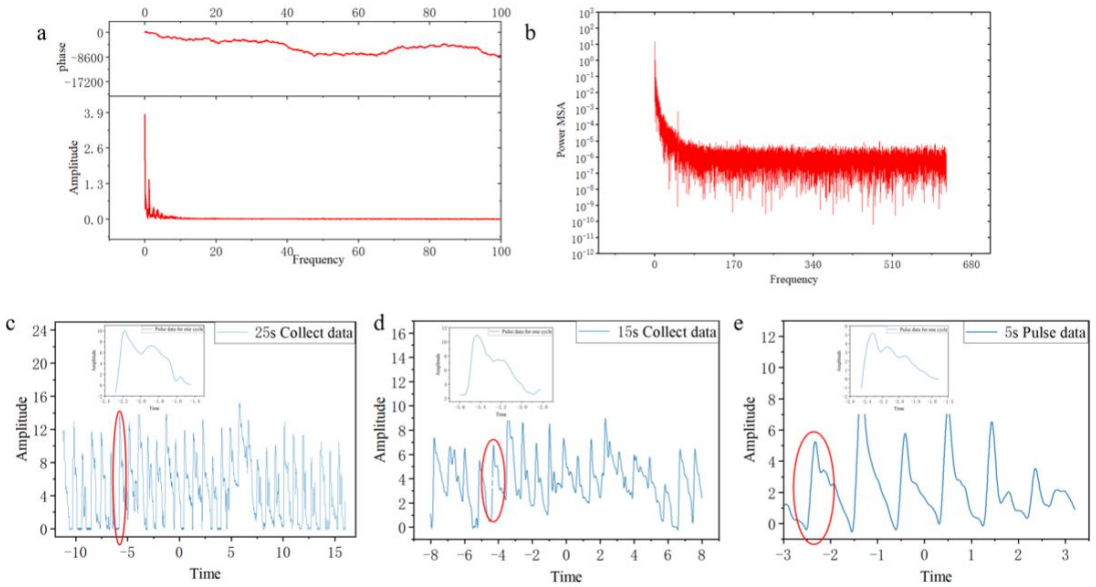

Figure 3.The following is a revised version: The pulse signal exhibits frequency domain variation, with the majority of its energy concentrated below 5 Hz. (a) Fourier variation graph; (c) pulse signal acquisition graphs of 25 s with one cycle; (d) 15 s with one cycle; (e) 5 s with one cycle.

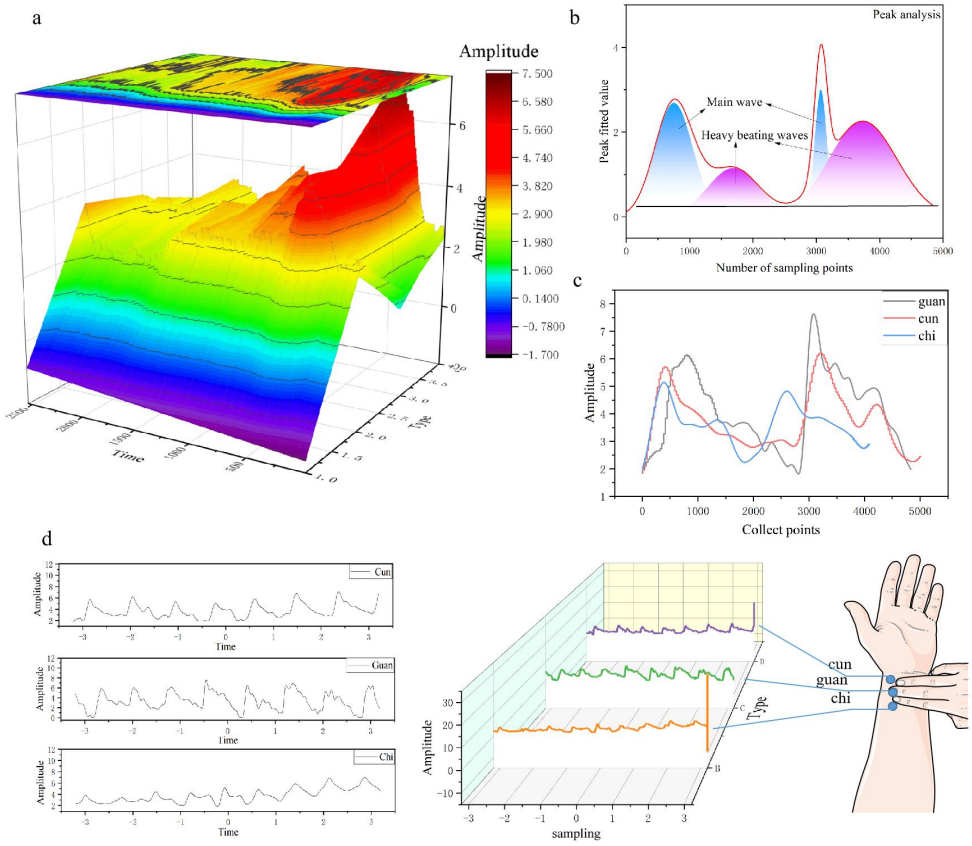

Figure 4. (a) 3D pulse signals from Cun, Guan, and Chi; (b) comparison of the areas of the main wave and the reboot wave for the Cun and Guan signal; (c) the differences between Cun, Guan, and Chi at the same time; (d) Three places on the human wrist (Cun, Guan, and Chi) to measure and display the pulse signals with a waterfall plot for each segment vs each of the three signals.

sample in the training set, random panning amounts and scaling factors are generated and applied to generate two new samples. The translation amount is a randomly generated integer ranging from -500 to 500, whereas the scaling factor is a random floating point number ranging from 0.5 to 1.5. This type of data augmentation enhances the diversity and robustness of training samples. Once the above preprocessing tasks are complete, the CNN model, which comprises three convolutional layers, three maximum pooling layers, a spreading layer, a fully connected layer, and an output layer (shown in Fig. 5) is built and trained. The specific method is also shown in Fig. 6.

The pulse wave data stored in each file undergoes conversion into a two-dimensional array, representing the two distinctive dimensions of the graphene pulse signal - time and pulse wave. A label is assigned to each set of data based on the name of the subfolder that stores the file, indicating the signal category. In order to maintain data consistency, only the first 15,000 time points are considered for the datasets that have a length exceeding 15,000 time points. For datasets shorter than 15,000 time points, zero-padding is applied to achieve the same length.

For each data point, filter smoothing is achieved by using the moving average method. The moving average window is set to 100. Baseline drift removal is accomplished by a third-order polynomial fitting, and then are subtracted from the original data. The results are shown in Fig. 6. The filtering and baseline drift removal effects are evident in the results.

Based on the experimental analysis of pulse wave data, the classification model for CNN pulse wave recognition achieved a final training set accuracy of 85.79% and a test set accuracy of 80%.

4. Conclusion

This paper presents a novel platform for pulse sensing based on paper-based graphene flexible sensors with high sensitivity and conductivity. The platform achieves stable acquisition of pulse waves under continuously varying pressure. We explore signal characteristics at three pulse locations (Cun, Guan, and Chi) by detecting, recording pulse signals and analyzing the characteristic points of the signals. Machine learning are used to classify and process the signals in motion, culminating in high accuracy rates of 85.79% for the training set and 80% for the test set. Overall, the study offers valuable insights for the development of practical applications in the field of flexible material design and wearable electronics, particularly in relation to personal health care and the Internet of Things.

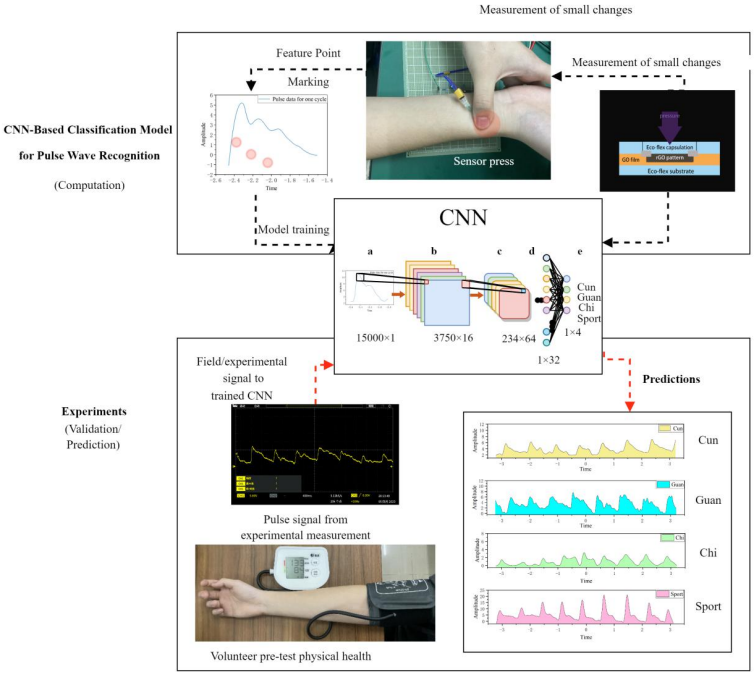

Figure 5 Overview of the proposed method. The CNN is fully trained using pulse signal data (top). The simulated trained CNN is then applied to classify (Cun, Guan, Chi and Sport) four classes of signals (bottom). (a) Input layer ;(b) Convolutional layers; (c) Pooling layer ;(d) Fully connected layer; (e) Output layer;

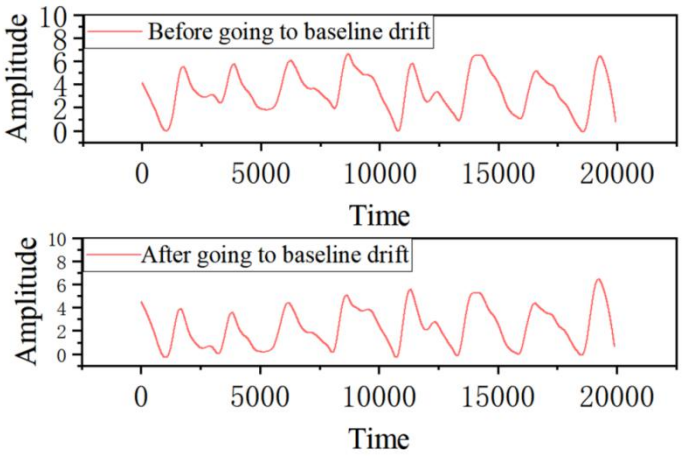

Figure 6 Data baseline drift processing: before de-baseline drift (top); after de-baseline drift (bottom).

References

[1] Khan Y, Ostfeld A E, Lochner C M, et al. Monitoring of vital signs with flexible and wearable medical devices[J]. Advanced materials, 2016, 28(22): 4373-4395.

[2] Rim Y S, Bae S H, Chen H, et al. Recent progress in materials and devices toward printable and flexible sensors[J]. Advanced Materials, 2016, 28(22): 4415-4440.

[3] Chung Y F, Hu C S, Yeh C C, et al. How to standardize the pulse-taking method of traditional Chinese medicine pulse diagnosis[J]. Computers in biology and medicine, 2013, 43(4): 342-349.

[4] Tang Y, Huang F, Bi H, et al. Highly conductive three-dimensional graphene for enhancing the rate performance of LiFePO4 cathode[J]. Journal of Power Sources, 2012, 203: 130-134.

[5] Di Bartolomeo A. Graphene Schottky diodes: An experimental review of the rectifying graphene/semiconductor heterojunction[J]. Physics Reports, 2016, 606: 1-58.

[6] X. Li, W. Cai, J. An, S. Kim, J. Nah, D. Yang, R. Piner, A. Velamakanni, I. Jung, E. Tutuc, S.K. Banerjee, L. Colombo, R.S. Ruoff, Large-area synthesis of high-quality and uniform graphene films on copper foils, Science (80-.). 324 (2009) 1312–1314. doi:10.1126/science.1171245.

[7] Kan-heng, Z.; Peng, Q.; Chun-ming, X.; Yi-qin, W. Research on a Novel Three-Channel Self-Pressurized Wrist Pulse Acquisition System. In Biomedical Engineering Systems and Technologies; Springer: Berlin/Heidelberg, Germany, 2015; pp. 49–59.

[8] Tao, L. Q., K. N. Zhang, H. Tian, Y. Liu, D. Y. Wang, Y. Q. Chen, Y. Yang and T. L. Ren (2017). "Graphene-Paper Pressure Sensor for Detecting Human Motions." ACS Nano 11(9): 8790-8795.

[9] Li G, Watanabe K, Anzai H, et al. Pulse-wave-pattern classification with a convolutional neural network[J]. Scientific reports, 2019, 9(1): 14930.

[10] Li X, Huang Z, Wang F, et al. Toward convolutional neural networks on pulse repetition interval modulation recognition[J]. IEEE Communications Letters, 2018, 22(11): 2286-2289.

[11] Lee M S, Lee Y K, Pae D S, et al. Fast emotion recognition based on single pulse PPG signal with convolutional neural network[J]. Applied Sciences, 2019, 9(16): 3355.

[12] Marcano D C, Kosynkin D V, Berlin J M, et al. Improved synthesis of graphene oxide[J]. ACS nano, 2010, 4(8): 4806-4814.

[13] Motaghi, A., Hrymak, A., & Motlagh, G. H. (2015). Electrical conductivity and percolation threshold of hybrid carbon/polymer composites. Journal of applied polymer Science, 132(13).

[14] Hassan, H.; Kim, H.-W. CMOS Capacitive Fingerprint Sensor Based on Differential Sensing Circuit with Noise Cancellation. Sensors 2018, 18, 2200.

[15] Wu X, Yang X, Jin J, et al. Amplitude-based filtering for video magnification in presence of large motion[J]. Sensors, 2018, 18(7): 2312.

[16] Shibasaki, M.; Namba, M.; Oshiro, M.; Kakigi, R.; Nakata, H., Suppression of cognitive function in hyperthermia; From the viewpoint of executive and inhibitive cognitive processing. Scientific reports 2017, 7 (1), 1-8.

[17] Differences in the Properties of the Radial Artery between Cun, Guan, Chi, and Nearby Segments Using Ultrasonographic Imaging: A Pilot Study on Arterial Depth, Diameter, and Blood Flow)